PERGAMON

Deep-Sea Research II 49 (2002) 707–721

DEEP-SEA RESEARCH
PART II

www.elsevier.com/locate/dsr2

Photosynthesis, primary production and phytoplankton growth rates in Gerlache and Bransfield Straits during Austral summer: cruise FRUELA 95

Luisa M. Lorenzo[a,*], Belén Arbones[a], Francisco G. Figueiras[a], Gavin H. Tilstone[a,1], Félix L. Figueroa[b]

[a] *CSIC, Instituto de Investigacións Mariñas, Eduardo Cabello, 6. 36208 Vigo, Spain*
[b] *Dep. Ecología (Facultad de Ciencias), Universidad de Málaga, Campus de Teatinos s/n 29071-Malaga, Spain*

Received 25 July 2000; received in revised form 4 December 2000; accepted 6 January 2001

Abstract

Bio-optical parameters, primary production, and phytoplankton growth rates were determined in the southern part of the Bellingshausen Sea, the western part of the Bransfield Strait, and the Gerlache Strait, during December 1995 and early January 1996. Three water bodies were present at the surface ($<100\,$m); Bellingshausen warm waters (BWW), Bellingshausen cold waters (BCW), and transitional Weddell waters (TWW), which were separated by a thermal front. High chlorophyll concentrations were found in the upper mixed layer (UML) of the BCW waters ($5.57\pm4.04\,\mathrm{mg\,m^{-3}}$), with intermediate values in BWW ($2.85\pm1.24\,\mathrm{mg\,m^{-3}}$) and the lowest values in the TWW ($1.53\pm0.94\,\mathrm{mg\,m^{-3}}$). The broadband photosynthetic parameters ($P^{\mathrm{B}}_{\max}$, α^{B} and $E_{K\mathrm{PAR}}$) were highest in BWW and lowest in TWW, except for $E_{K\mathrm{PAR}}$, which did not show significant differences between water bodies. Spectral bio-optical parameters ($\overline{a_{\mathrm{ph}}}$, $\phi_{\max}$ and $E_{K\mathrm{PUR}}$) showed a similar distribution to chlorophyll concentrations except $E_{K\mathrm{PUR}}$, which was highest in BWW. A comparison between light-saturation parameters and water-column irradiance suggests that photosynthesis was not light-limited in the mixed layer. However, transitory situations exist where photosynthesis could be close to limitation at the bottom of the photic layer when high chlorophyll concentrations were present in the surface layers. The high maximum quantum yields ($0.073\pm0.032\,$mol C (mol photons)$^{-1}$) also suggest that iron limitation of photosynthesis should not be occurring in the region during the cruise. The mean primary production rates were $1.11\pm0.68\,$g $\mathrm{C\,m^{-2}\,d^{-1}}$ in the TWW, $2.28\pm0.98\,$g $\mathrm{C\,m^{-2}\,d^{-1}}$ in the BCW, and $2.68\pm0.94\,\mathrm{g\,C^{-2}\,d^{-1}}$ in the BWW. The Gerlache Strait and frontal zones were the most productive, with values analogous to those of upwelling areas. Carbon-specific growth rates in UML ($0.43\pm0.16\,\mathrm{d^{-1}}$) were similar to those of temperate seas, neither nutrient- nor light-limited. Growth rates in the UML of BCW ($0.54\pm0.20\,\mathrm{d^{-1}}$) were higher than those of TWW ($0.37\pm0.08\,\mathrm{d^{-1}}$) and BWW ($0.35\pm0.09\,\mathrm{d^{-1}}$). The results indicate that factors as microzooplankton grazing or sinking should control the standing stock of phytoplankton, since photosynthesis was not limited.

1. Introduction

Traditionally the Antarctic ecosystem has been characterised as a zone of high-nutrient and low-chlorophyll conditions, which constitutes "the

---

*Corresponding author. Fax: +34-986-292762.
E-mail address: luimar@iim.csic.es (L.M. Lorenzo).

[1] Plymouth Marine Laboratory, Prospect Place West Hoe, Plymouth PL1 3DH, UK.

0967-0645/01/$ - see front matter © 2001 Elsevier Science Ltd. All rights reserved.
PII: S0967-0645(01)00120-5

major biological paradox of the Southern Oceans" (El-Sayed, 1987). Several authors, however, have shown that although phytoplankton biomass over the whole region may be relatively low, in some areas high phytoplankton biomass can be found associated with low water-column mixing or continental shelf waters but usually without nutrient depletion (El-Sayed, 1988; Holm-Hansen et al., 1989; Mitchell and Holm-Hansen, 1991; Sullivan et al., 1993). Limited phytoplankton activity due to low light levels (Sakshaug and Holm-Hansen, 1984), low temperatures (Smith and Sakshaugh, 1990) and iron deficiency (Martin et al., 1990), are the common reasons invoked to explain why nutrients are not totally exhausted.

The low light levels in the well-mixed surface layer of the Antarctic have been suggested as one of the most important factors controlling phytoplankton biomass (Sakshaug and Holm-Hansen, 1984). Nevertheless, during the Austral summer, solar irradiance in the UML is not generally considered to be limiting (Krebs, 1983; Holm-Hansen and Mitchell, 1991, Figueiras et al., 1994, 1998). An analysis of photosynthetic response to photosynthetic active radiation (PAR) and to photosynthetic usable or absorbed radiation by phytoplankton (PUR) in the water column, based on broad-band and spectral models, has shown that phytoplankton is light-saturated during the Austral summer (Figueiras et al., 1999). These observations may be true over broad latitudinal scales, but there is a large amount of hydrographic variability in Antarctic waters, which requires a more detailed analysis of phytoplankton light limitation, especially during transitional hydrographic situations at coastal and frontal zones.

The following paper presents a detailed analysis of photosynthetic parameters, primary production, and phytoplankton growth rates in the southern part of the Bellingshausen Sea, the western part of the Bransfield Strait, and the Gerlache Strait, a very dynamic region where the confluence of the Bellignshausen and Weddell waters occurs. For each water body, phytoplankton photosynthesis, primary production and phytoplankton growth rates were analysed in relation to surface mixed layer depths and irradiance, and the photoadaptational status was assessed in order to establish whether physiological limitation of phytoplankton occurred and was therefore responsible for the relatively low phytoplankton standing stocks usually found in the area.

2. Materials and methods

2.1. Sampling

The sampling area (Fig. 1) was the southern part of the Bellingshausen Sea, the western part of the Bransfield Strait, and the Gerlache Strait. The cruise (FRUELA 95) took place between 3 December 1995 and 5 January 1996 aboard the R/V *Hespérides* and was divided in two legs. During the first leg (3–11 December 1995) the hydrographic structure in the area was characterised. From the 47 stations sampled, 33 (Stns. 1–33, Fig. 1) were located in five perpendicular transects to the Antarctic Peninsula and 13 (Stns.

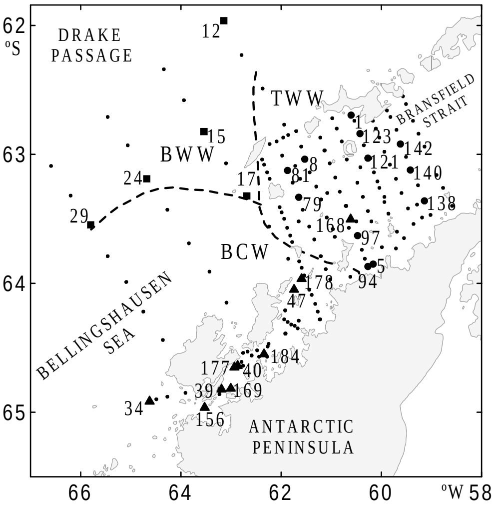

Fig. 1. Map of the sampling area showing CTD, stations (small circles) and bio-optical stations (larger circles, squares and triangles) where sampling was done. The dash line separates the three water bodies present in the area: Bellingshausen warm waters (BWW, ■), Bellingshausen cold waters (BCW, ▲), and transitional Weddell waters (TWW, ●). Station 168 was included in BCW for bio-optical analysis. See text for details.

34–47, Fig. 1) in the Gerlache Strait. The second leg (12 December 1995–5 January 1996) sampled the western basin of the Bransfield Strait where three water bodies meet (Fig. 1). This dense sampling grid (107 stations, Stns. 48–155, Fig. 1) was defined to establish the confluence boundaries of water bodies. At the end of the second leg, stations in the Gerlache Strait (28 stations, Stns. 156–184) were re-visited between 19 December 1995 and 5 January 1996, to detail the key processes that result in high chlorophyll concentrations in the region. Biological sampling was conducted at 27 stations (large numbered circles in Fig. 1) to determine phytoplankton light absorption and photosynthetic parameters and to estimate primary production and phytoplankton growth rates. Water samples were collected on the upcasts of a Mk IIIC Neil Brown CTD using 121 PVC Niskin bottles from the rosette.

2.2. Chlorophyll and phytoplankton light absorption coefficients

Chlorophyll *a* (Chl *a*) concentrations were estimated fluorometrically by pigment extraction in 90% acetone after filtering between 50 and 100 ml of seawater through 25-mm Whatman GF/F filters (Yentsch and Menzel, 1963). Fluorometer was calibrated against Chl *a* concentrations determined spectrophotometrically during the same cruise.

Phytoplankton light absorption coefficients ($a_{\mathrm{ph}}(\lambda)$, m^{-1}) were determined by filtering seawater volumes of 1–41 through 25 mm Whatman GF/F filters. The optical density spectra of concentrated material were measured on a Kontron UVIKON 860 dual-beam spectrophotometer at 1 nm bandwidth from 400 to 750 nm, using a wet GF/F filter as a blank. Phytoplankton pigments were extracted in methanol (Kishino et al., 1985), and the optical density of non-algal material retained on the filters was determined in the same way. Absorbance at 750 nm was subtracted from all other wavelengths in the spectra and the correction for pathlength amplification on filters was done following the methodology of Arbones et al. (1996).

2.3. Incident irradiance at the sea surface and light in the water column

The incident photosynthetically active radiation (PAR, $\lambda = 400-700\,\mathrm{nm}$) at the sea surface was measured on deck, at 1-min intervals, with a Li-Cor cosine corrected LI-190SA sensor. Readings were integrated hourly. Incident irradiance in Antarctica shows high short-term variability due to the rapid passing of clouds, which makes the interpretation of bio-optical results difficult (Figueiras et al., 1999). To remove this "noise" and allow a more generalised interpretation, the incident irradiance was averaged to obtain the mean PAR daily irradiance (E_{0+}) of 32 mol photons $\mathrm{m}^{-2}\,\mathrm{d}^{-1}$. Profiles of PAR irradiance were determined using a Biospherical radiometer (PUV500). The average transmittance at the air–sea interface ($\tau = 0.7$) was estimated from in situ measurements taken just above (E_{0+}) and below (E_{0-}) the sea surface. The mean daily PAR irradiance below the sea surface ($\overline{E_{0-}}$) was therefore estimated as follows:

$$\overline{E_{0-}} = \overline{E_{0+}}0.7 \tag{1}$$

and the PAR irradiance at each depth ($E_z\mathrm{PAR}$, µmol photons $\mathrm{m}^{-2}\,\mathrm{s}^{-1}$) in the water column as

$$E_z\mathrm{PAR} = E_{0-}\exp(-K_{\mathrm{PAR}}Z), \tag{2}$$

where K_{PAR} (m^{-1}) is the light attenuation coefficient for the PAR spectrum (400–700 nm).

The mean PAR irradiance (E_{UMLPAR}) in the UML is

$$E_{\mathrm{UMLPAR}} = 1/Z_{\mathrm{UML}} \int_0^{Z_{\mathrm{UML}}} \overline{E_{0-}} \times \exp(-K_{\mathrm{PAR}}Z)\,\mathrm{d}z, \tag{3}$$

where the depth of the UML (Z_{UML}) was estimated assuming that a change of $\sigma_t \geqslant 0.05$ over 5 m depth interval defines the pycnocline (Mitchell and Holm-Hansen, 1991).

The spectral incident irradiance at the sea surface and in the water column was determined with a Li-1800 spectra-radiometer. Measurements in the water column were taken at 5–10 m intervals. To study temporal and spatial variations in the shape of the spectra during the cruise, midday spectra above and just below the sea surface were normalised to its integral and then correlated. Correlation of normalised incident spectra at the sea surface was high ($0.87 < r^2 < 0.94$), and the linear regression slopes varied between 0.997 and 1.006, which indicates that the shape of incident spectra during midday did not change significantly throughout the cruise. The average midday normalised spectra above and just below the surface also showed a high correlation ($r^2 = 0.90$), with a slope of 1.006, indicating that the transmittance through the air–water interface was constant and independent of wavelength (Kirk, 1983; Falkowski and Raven, 1997). Nevertheless, differences were found in the shape of the normalised spectra during the day (Fig. 2), with blue light being more important at dawn and dusk. These differences, however, have no effect on integrated primary production (see Eq. (13)) when calculated considering the shape of the midday irradiance spectra or using the correspond real shape of spectra at dawn and dusk ($r^2 = 0.99$, slope $= 0.99 \pm 0.0005$, $P = 0.25$ for paired samples). This, therefore, allows us to use a single spectral shape of incident light during the entire cruise as well as a constant PAR transmittance coefficient ($\tau = 0.7$) through the air–sea interface.

The average light spectrum just below the sea surface was estimated from

$$\overline{E_{0-}(\lambda)} = \overline{E_{0-}}\,\overline{E_{N0+}(\lambda)}, \tag{4}$$

where $\overline{E_{0-}}$ is the mean PAR irradiance below the sea surface calculated using Eq. (1), and $\overline{E_{N0+}(\lambda)}$ is the average of the normalised spectra at the sea surface.

The spectral irradiance at each depth in the water column ($E_z(\lambda)$, μmol photons $\mathrm{m}^{-2}\,\mathrm{s}^{-1}$) was estimated as

$$E_z(\lambda) = \overline{E_{0-}(\lambda)}\exp(-K(\lambda)Z) \tag{5}$$

and the spectral light absorbed by phytoplankton at each depth ($E_{z\mathrm{PUR}}$, μmol photons $\mathrm{m}^{-3}\,\mathrm{s}^{-1}$) is

$$E_{z\mathrm{PUR}} = \int_{400}^{700} a_{\mathrm{ph}}(\lambda)E_z(\lambda)\,\mathrm{d}\lambda, \tag{6}$$

where $a_{\mathrm{ph}}(\lambda)$ (m^{-1}) is the phytoplankton spectral absorption coefficient.

The mean irradiance absorbed by phytoplankton in the UML (E_{UMLPUR}) is

$$E_{\mathrm{UMLPUR}} = 1/Z_{\mathrm{UML}}\int_{0}^{Z_{\mathrm{UML}}} E_{z\mathrm{PUR}}(z)\,\mathrm{d}z. \tag{7}$$

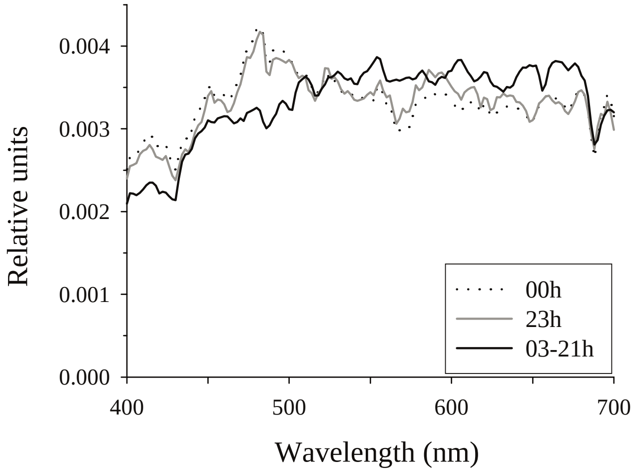

Fig. 2. Normalised spectra during different times. The biggest differences were found between the spectra measured at dawn and dusk (00 and 23 h) with the ones measured during light hours (03–21 h).

2.4. Photosynthesis-irradiance relationships

Fourteen subsamples collected in 75-ml Corning tissue culture flasks were inoculated with 3.70×10^5 Bq (10 μCi) of ^{14}C-labelled bicarbonate and placed in linear incubators illuminated by tungsten–halogen lamps (50 W, 12 V) of a known light spectra. The flask at the end of the incubator was covered with aluminium foil and used to check dark carbon fixation. A digital temperature refrigeration unit was used to maintain the samples at ambient temperature. The PAR (E_{PAR}) at the position of each bottle in the incubators was measured with a Li-Cor cosine sensor LI-190SA. After 2 h of incubation, samples were filtered through 25 mm Whatman GF/F filters. The filters were exposed to concentrated HCl fumes for 12 h to eliminate unincorporated ^{14}C. The external standard and the channel ratio methods were used to calculate disintegrations per minute (dpm).

Since photoinhibition was not observed, the broadband photosynthetic parameters, $P_{\mathrm{m}}^{\mathrm{B}}$ (mg C(mg Chl)$^{-1}$ h^{-1}) and α^{B} (mg C(mg Chl)$^{-1}$ h^{-1} (μmol m^{-2} s^{-1})$^{-1}$) were estimated by fitting the data to the model of Webb et al. (1974):

$$P_z^{\mathrm{B}} = P_{\mathrm{m}}^{\mathrm{B}}[1-\exp(-\alpha^{\mathrm{B}}E_{\mathrm{PAR}}/P_{\mathrm{m}}^{\mathrm{B}})], \tag{8}$$

where P_z^{B} (mg C(mg Chl)$^{-1}$ h^{-1}) is the Chl-specific rate of photosynthesis at each sampled depth.

The spectral quality of the incident light did not change along the incubators (Figueiras et al., 1999), and therefore the spectral irradiance $E_q(\lambda)$ at each location in the incubators was deduced by multiplying the normalised spectra of the tungsten–halogen lamp $E_{\mathrm{N}}(\lambda)$ by the corresponding E_{PAR} at each location:

$$E_q(\lambda) = E_{\mathrm{N}}(\lambda)E_{\mathrm{PAR}}, \tag{9}$$

where

$$E_{\mathrm{N}}(\lambda) = E(\lambda)/\int_\lambda E(\lambda)\,\mathrm{d}\lambda. \tag{10}$$

The light absorbed by phytoplankton (E_{PUR}, μmol photons m^{-3} s^{-1}) at each position in the incubators was calculated following Dubinsky (1980):

$$E_{\mathrm{PUR}} = \int_{400}^{700} a_{\mathrm{ph}}(\lambda)E_q(\lambda)\,\mathrm{d}\lambda. \tag{11}$$

The maximum quantum yield of carbon fixation (ϕ_{m}, mol C fixed (mol photons absorbed)$^{-1}$) was estimated by fitting the photosynthetic rates P (mg C m^{-3} h^{-1}) to the photosynthetic radiation absorbed by phytoplankton E_{PUR} (μmol photons m^{-3} s^{-1}):

$$P_z = P_{\mathrm{m}}[1-\exp(-\phi_m' E_{\mathrm{PUR}}/P_{\mathrm{m}})], \tag{12}$$

where $\phi_{\mathrm{m}} = 0.0231\phi_{\mathrm{m}}'$. The factor 0.0231 converts milligrams of carbon to moles, μmol of photons to moles, and hours to seconds.

From Eq. (12) the spectral light saturation parameter for light absorbed by phytoplankton ($E_{K\mathrm{PUR}} = P_{\mathrm{m}}/\phi_m'$, (μmol photons m^{-3} s^{-1})), is analogous to the saturation parameter for PAR radiation ($E_{K\mathrm{PAR}} = P_{\mathrm{m}}^{\mathrm{B}}/\alpha^{\mathrm{B}}$, (μmol photons m^{-2} s^{-1})) derived from broadband photosynthesis—irradiance relationships.

2.5. Primary production and phytoplankton carbon-specific gross growth rates

Primary production (PP) was integrated to the depth of 1% of surface irradiance ($Z_{1\%}$):

$$\mathrm{PP} = D\int_0^{Z_{1\%}} \mathrm{chl}(z)P_{\mathrm{m}}^{\mathrm{B}}(z) \times \left[1-\exp(-E_{\mathrm{PUR}}(z)/E_{K\mathrm{PUR}}(z))\right]\mathrm{d}z, \tag{13}$$

where the daylength D is 24 h.

Gross phytoplankton growth rates ($\mu + r$, d^{-1}, where μ represents the net growth rate and r the respiration rate) were calculated as

$$\mu + r = \ln\left[1+\frac{\mathrm{d}C/\mathrm{d}t}{C}\right], \tag{14}$$

where $\mathrm{d}C/\mathrm{d}t$ is the daily integrated PP (mg C m^{-3} d^{-1}) at each depth:

$$\mathrm{d}C/\mathrm{d}t = D\mathrm{Chl}P_{\mathrm{m}}^{\mathrm{B}}[1-\exp(E_{z\mathrm{PUR}}/E_{K\mathrm{PUR}})] \tag{15}$$

and C (mg C m^{-3}) is the phytoplankton carbon estimated from the slope of the linear regression (model II) between particulate organic carbon

(POC, see Doval et al., 2002) and Chl:

$$\mathrm{POC} = 26.96(\pm 4.4) + 53.63(\pm 1.8)\,\mathrm{Chl} \quad (r^2 = 0.75,\ n = 228). \tag{16}$$

This carbon : chlorophyll ratio is similar to that reported previously for a nearby area (Figueiras et al., 1994) and compares well with that found for Antarctic phytoplankton growing in culture (Thomas et al., 1992).

3. Results and discussion

3.1. Hydrographic regions

Surface waters (<100 m) in the Bellingshausen Sea and in the Gerlache Strait were occupied by transitional Bellingshausen waters (TBW), while in the Bransfield Strait, transitional Weddell waters (TWW) dominated (Garcia et al., 2002). However, within surface TBW (<70 m) there were two water bodies (Tokarczyk, 1987): Bellingshausen warm waters (BWW) and Bellingshausen cold waters (BCW) (see Fig. 1), which had a similar salinity range (33.1–33.9 psu in summer) and were differentiated by temperature. The BWW, with temperatures above 0.5°C, occupied the upper 50–75 m of the water column in the northwestern part of the study area and influenced the Drake Passage waters. The BCW, which were colder than BWW, were located at the southwestern in the upper 30–50 m. The BCW penetrated from the west, through the Gerlache Strait, to reach the Bransfield Strait where it met the TWW. TWW was characterised by temperatures below -1.5°C and salinity between 33.6 and 34.6 psu in summer; consequently, TWW had a higher density than BCW and, therefore, occurred below BCW in the western part of the Bransfield Strait (Fig. 1). A thermal front characterised by the 0°C isotherm located between Drake Passage and Bellingshausen Sea corresponded to a separation between warm BWW from the BCW and cold TWW. The front accumulated chlorophyll with averaged concentrations in the mixed layer >2 mg Chl $a\,\mathrm{m}^{-3}$ (Castro et al., 2002). The stations were assigned to each hydrographic region, according to their geographic position (Fig. 1), with the exception of station 168, which presented surface waters with BCW characteristics when the bio-optical samplig was carried out, and was included in the BCW group.

The water-column structure did not show a differentiated pattern according to the water bodies distribution. Stations with relatively deep UML (e.g., Stns. 142 and 40, Fig. 3) were found in TWW and BCW, where stratified water columns also were observed (e.g. Stns. 1 and 178, Fig. 3). Stratified stations ($Z_{UML} < 10$ m) were usually found in the Gerlache Strait (BCW) and at some coastal stations for the TWW. At stations with shallow UML the photic layer was deeper than Z_{UML}. The stations in BWW did not show any evidence of stratification; their UML was around 40 m deep (e.g. Stn. 12, Fig. 3) and their photic layer was shallower than Z_{UML}.

3.2. Chlorophyll

The average Chl a concentration in the water column at stations where $P-E$ measurements were made was 2.86 ± 2.50 mg Chl $a\,\mathrm{m}^{-3}$. By comparison, Holm-Hansen and Mitchell (1991) found a mean value of 6.5 ± 4.7 mg Chl $a\,\mathrm{m}^{-3}$ for the same area and season, with the highest Chl a concentrations at surface waters in the Gerlache Strait (>10 mg Chl $a\,\mathrm{m}^{-3}$) associated with the shallowest UMLs ($Z_{UML} < 20$ m). We also observed a similar Chl a pattern in this zone, but with lower concentrations at the surface (Chl $a > 3\,\mathrm{mg\,m}^{-3}$) and shallower mixed layers ($Z_{UML} < 10$ m). The mean Chl a concentration of BCW waters was higher than that of the other two water bodies, especially in the UML (Tables 1 and 2). Chl a concentrations at the surface layer of stratified stations, in BCW especially, were higher than in TWW (Table 1).

3.3. Photosynthetic broadband parameters

The mean and standard deviation of broadband photosynthetic parameters ($P^{\mathrm{B}}_{\mathrm{m}}$, α^{B} and $E_{K\mathrm{PAR}}$) in each hydrographic region and for all samples are given in Table 1. The overall mean maximum photosynthetic rate $P^{\mathrm{B}}_{\mathrm{m}}$ (2.16 ± 1.09 mg C (mg

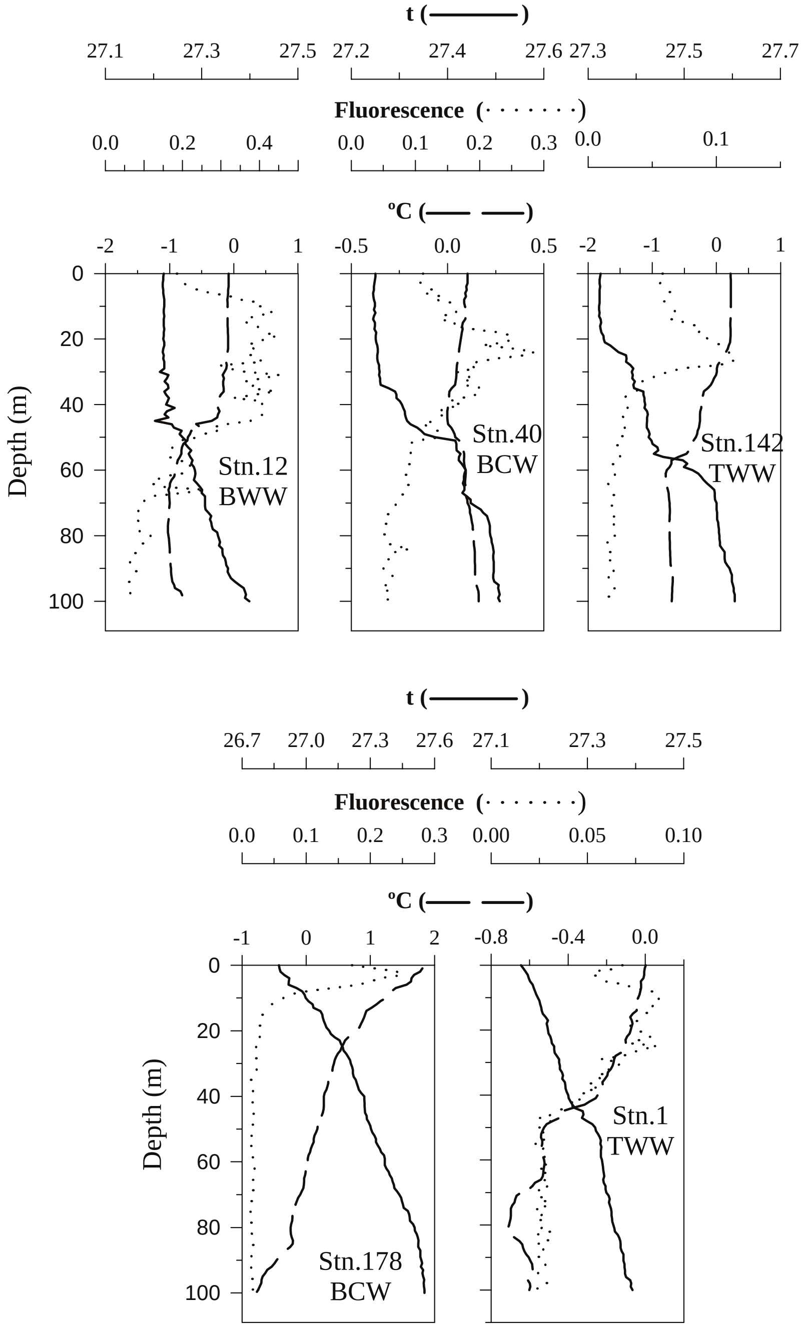

Fig. 3. Vertical profiles of temperature, fluorescence and σ_t of selected stations from BWW, BCW and TWW. Stations 12, 40 and 142 showed vertical mixing. Stratified water column conditions were observed in stations 178 and 1.

Table 1
Mean and standard deviation of chlorophyll concentration (Chl), broadband photosynthetic parameters (P^B_m, α^B, E_{KPAR}) and bio-optical parameters ($\overline{a_{ph}}$, E_{KPUR}, ϕ_m) in the water column (Total) of the three water bodies found in the area (BCW, BWW, TWW), layers in the water column (UML, B_{UML}) and or total samples[a]

Water bodies	Layer	Chl	P^B_m	α^B	E_{KPAR}	$\overline{a_{ph}}$	E_{KPUR}	ϕ_m
BCW	Total	4.34±3.39	2.19±0.95	0.040±0.013	56±27	0.066±0.055	2.4±1.7	0.088±0.029
	UML	5.57±4.04	2.29±0.90	0.040±0.019	59±26	0.094±0.062	3.1±1.9	0.089±0.019
	B_{UML}	2.65±0.82	2.06±1.06	0.039±0.018	53±30	0.032±0.010	1.5±0.9	0.086±0.040
BWW	Total	2.85±1.24	3.21±1.23	0.044±0.011	79±40	0.054±0.045	3.8±3.9	0.087±0.038
	UML	2.85±1.24	3.21±1.23	0.044±0.011	79±40	0.054±0.045	3.8±3.9	0.087±0.038
	B_{UML}	—	—	—	—	—	—	—
TWW	Total	1.64±1.02	1.69±0.81	0.037±0.018	50±23	0.036±0.024	1.2±0.7	0.055±0.023
	UML	1.53±0.94	1.59±0.54	0.032±0.010	55±28	0.032±0.018	1.1±0.6	0.050±0.021
	B_{UML}	1.79±1.15	1.82±1.08	0.043±0.025	43±12	0.041±0.030	1.2±0.9	0.061±0.026
Total samples		2.86±2.50	2.16±1.09	0.039±0.015	58±30	0.048±0.041	2.1±2.2	0.073±0.032

[a] BCW, Bellingshausen cold waters; BWW, Bellingshausen warm waters; TWW, transitional Weddell waters; UML, upper mixed layer; B_{UML} below upper mixed layer but within photic layer (UML of BWW were deeper than photic layers). Chl (mg m^{-3}); P^B_m (mg C (mg Chl)$^{-1}$ h^{-1}); α^B (mg C (mg Chl)$^{-1}$ h^{-1} (μmol m^{-2} s^{-1})$^{-1}$); E_{KPAR} (μmol photons m^{-2} s^{-1}); $\overline{a_{ph}}$ (m^{-1}); E_{KPUR} (μmol photons m^{-3} s^{-1}); ϕ_m (mol C (mol photons)$^{-1}$)

Table 2
Results of comparisons (probability of *t*-tests) between layers (UML, B_{UML}) and water bodies (BCW, BWW, TWW) for chlorophyll (Chl), broadband photosynthetic parameters (P^B_m, α^B, E_{KPAR}) and bio-optical parameters ($\overline{a_{ph}}$, E_{KPUR}, ϕ_m) on Table 1[a]

Layer or water body	Comparison	Chl	P^B_m	α^B	E_{KPAR}	$\overline{a_{ph}}$	E_{KPUR}	ϕ_m
UML	BWW–TWW	0.01	<0.001	0.01	0.11	0.16	0.03	0.01
	BWW–BCW	0.06	0.06	0.37	0.20	0.18	0.63	0.87
	TWW–BCW	0.002	0.03	0.04	0.63	0.01	0.002	<0.001
B_{UML}	BCW–TWW	0.10	0.64	0.70	0.36	0.52	0.55	0.12
BCW	UML–B_{UML}	0.06	0.61	0.88	0.64	0.06	0.04	0.86
TWW	UML–B_{UML}	0.55	0.51	0.14	0.24	0.39	0.86	0.25

[a] $P \leqslant 0.05$ significant at the 95% level; $P \leqslant 0.01$ significant at the 99% level and $P \leqslant 0.001$ significant at the 99.9% level.

Chl)$^{-1}$ h^{-1}) was slightly higher than that reported by other authors (e.g. Tilzer et al., 1985; Holm-Hansen and Mitchell, 1991; Figueiras et al., 1994, 1998) but within the range found by Sakshaug and Holm-Hansen (1986). The average broadband light-limited slope α^B (0.039±0.015 mg C (mg Chl)$^{-1}$ h^{-1} (μmol m^{-2} s^{-1})$^{-1}$) was also higher than that obtained by Tilzer et al. (1985) and Figueiras et al. (1998) but lower than values given by Holm-Hansen and Mitchell (1991) and Figueiras et al. (1994). The average P^B_m and α^B values were at the upper limit of the range given by Harrison and Platt (1986) for Arctic waters. The mean broadband light-saturation parameter (E_{KPAR}, 58±30 μmol m^{-2} s^{-1}) is also within the range reported previously for the Antarctic waters and was <100 μmol m^{-2} s^{-1}, which indicates low light adaptation by phytoplankton (Figueiras et al., 1998).

The three broadband photosynthetic parameters showed the lowest values in TWW, intermediate values in BCW, and the highest in BWW (Table 1).

For P_m^B and α^B the differences were only significant between TWW and the other two water bodies in the UML (Table 2). There were no significant differences between BWW and BCW, although P_m^B was close to the level of significance ($P = 0.06$, Table 2). However, in spite of these differences, the light broadband saturation parameter $E_{K\mathrm{PAR}}$ did not show significant changes between water bodies and layers (Table 2) and presented more similar values in the UML of TWW and BCW. The similarity of $E_{K\mathrm{PAR}}$ values was due to the covariation of P_m^B and α^B between water bodies. The low variability of $E_{K\mathrm{PAR}}$ in the region and the higher P_m^B and α^B in BCW and BWW than in TWW, imply that carbon fixation will be greater in BCW and BWW than in TWW for a given irradiance.

3.4. Bio-optical photosynthetic parameters

The mean spectral bio-optical parameters for all samples ($\overline{a_{\mathrm{ph}}}$, $E_{K\mathrm{PUR}}$, and ϕ_m, Table 1) were 4, 3 and 1.2 times higher than those found by Figueiras et al. (1999) for the nearby eastern Bransfield Strait in January 1994. The mean absorption coefficient ($\overline{a_{\mathrm{ph}}}$) of TWW in the UML was significantly lower than that of BCW (Table 2). There were also differences within the water column of BCW, with higher values in the UML (Tables 1 and 2). The same pattern occurred with $E_{K\mathrm{PUR}}$, but in this case the values in the UML of BCW and BWW were different to those in the UML in TWW (Tables 1 and 2). The highest $E_{K\mathrm{PUR}}$ values were found in BWW and the lowest in TWW (Table 1). TWW waters were vertically more homogeneous than BCW (Table 2), as was also observed in the Chl *a* distribution.

The mean maximum quantum yield (ϕ_m) was high (0.073 ± 0.032 mol C (mol photons)$^{-1}$), indicating no nutrient limitation for phytoplankton (Cleveland et al., 1989; Platt et al., 1992) as has been previously reported for this region (Figueiras et al., 1999). The highest values (> 0.073 mol C (mol photons)$^{-1}$) were found in BCW, at coastal stations in the Gerlache Strait. The lowest ϕ_m values were found in the homogenous TWW, where ϕ_m in the UML was significantly lower than those for BCW and BWW (Table 2). By contrast, there were no significant differences within the water column of BCW and TWW (Table 2). However, the mean ϕ_m (0.055 ± 0.023 mol C (mol photons)$^{-1}$) in TWW does not indicate neither macro-nutrient nor iron limitation of phytoplankton photosynthesis (Cleveland et al., 1989; Platt et al., 1992; Lindley et al., 1995).

3.5. Photosynthesis and light in the water column

Light limitation of photosynthesis has been suggested as one of the factors responsible for the low phytoplankton biomass usually found in well-mixed Antarctic waters (e.g., Sakshaug and Holm-Hansen, 1984). However, recently, several authors (Figueiras et al., 1994, 1998, 1999; Helbling et al., 1995) found no evidence of light limitation in the mixed surface layer. The data set presented here, which include areas with shallow UMLs and well stratified water columns with relatively high phytoplankton concentrations, enabled us to perform a more detailed analysis of light limitation in the Antarctic.

Light limitation of photosynthesis can be investigated by comparing the light received ($E_{z\mathrm{PAR}}$) and light absorbed ($E_{z\mathrm{PUR}}$) by phytoplankton against the corresponding light limitation parameters ($E_{K\mathrm{PAR}}$ and $E_{K\mathrm{PUR}}$, respectively). $E_{K\mathrm{PAR}}$ or $E_{K\mathrm{PUR}}$ greater than corresponding $E_{z\mathrm{PAR}}$ or $E_{z\mathrm{PUR}}$ values indicates light limitation in the water column. Table 3 shows the mean values of these four variables in the UML and below the UML ($\mathrm{B_{UML}}$), as well as the results of the statistical comparisons. In the UML, no significant differences were found between $\overline{E_{K\mathrm{PAR}}}$ and E_{UMLPAR}, but the differences were significant in $\mathrm{B_{UML}}$, where $\overline{E_{K\mathrm{PAR}}}$ was higher than $\overline{E_{z\mathrm{PAR}}}$, indicating light limitation when PAR radiation is considered. By comparison, the PUR parameters ($\overline{E_{K\mathrm{PUR}}}$ and E_{UMLPUR} or $\overline{E_{z\mathrm{PUR}}}$) did not show significant differences in any of the two layers, suggesting no light limitation of photosynthesis. However, $\overline{E_{K\mathrm{PUR}}}$ was slightly higher than $\overline{E_{z\mathrm{PUR}}}$ at the $\mathrm{B_{UML}}$ (Table 3), indicating that limitation of carbon fixation could occur in some locations. To analyse this further, in situ or operational quantum yields (ϕ) were compared against maximum quantum yields (ϕ_m). When photosynthesis is

Table 3
Mean and standard deviation of broadband ($\overline{E_{K\text{PAR}}}$) and spectral ($\overline{E_{K\text{PUR}}}$) light saturation parameters and the corresponding light received ($\overline{E_{\text{PAR}}}$) and light absorbed ($\overline{E_{\text{PUR}}}$) by phytoplankton in UML and B_{UML}[a]

Layer	$E_{K\text{PAR}}$	E_{PAR}	P	$E_{K\text{PUR}}$	E_{PUR}	P
UML	63±33	56±42	0.48	2.38±2.45	2.85±3.10	0.52
B_{UML}	48±22	25±36	0.03	1.35±0.89	1.17±1.99	0.61

[a] In UML $\overline{E_{\text{PAR}}}$ and $\overline{E_{\text{PUR}}}$ are the mean PAR (E_{UMLPAR}) and PUR (E_{UMLPUR}) irradiance estimated according to Eqs. (3) and (7), respectively. $\overline{E_{\text{PAR}}}$ and $\overline{E_{\text{PUR}}}$ in B_{UML} are the average of single values $\overline{E_{z\text{PAR}}}$ and $\overline{E_{z\text{PUR}}}$ estimated by Eqs. (2) and (6), respectively. P are the probabilities of t-tests for two samples (UML) and for paired samples (B_{UML}).

light-limited ϕ should be equal to ϕ_{m}, and when photosynthesis is light-saturated ϕ should be lower than ϕ_{m} (Figueiras et al., 1999).

The mean in situ quantum yields ($\overline{\phi_{\text{UML}}}$, mol C (mol photons)$^{-1}$) in the UML was estimated as follows:

$$\overline{\phi_{\text{UML}}} = \frac{1}{Z_{\text{UML}}} \int_0^{Z_{\text{UML}}} \text{PP}_z / E_{z\text{PUR}} \, \text{d}z, \qquad (17)$$

where PP_z is the daily integrated primary production at each depth in the UML (mol C m^{-3} d^{-1}) and $E_{z\text{PUR}}$ (mol photons m^{-3} d^{-1}) is the light absorbed by phytoplankton. Single values of ϕ were analysed for B_{UML}.

The operational quantum yields in the UML (mean 0.042±0.024 mol C (mol photons)$^{-1}$) were below ($P<0.001$, see also Fig. 4) the corresponding maximum quantum yields (mean 0.072±0.027 mol C (mol photons)$^{-1}$), indicating that photosynthesis was occurring at saturating light in the UML. Photosynthesis was also light-saturated in B_{UML} (Fig. 4) because operational quantum yields (mean 0.060±0.037 mol C (mol photons)$^{-1}$) were also significantly different ($P = 0.002$, t-test for paired samples) from maximum quantum yields (mean 0.075±0.035 mol C (mol photons)$^{-1}$). Nevertheless, some samples located at the lower limit of the B_{UML} layer showed ϕ almost equal to ϕ_{m} (Fig. 4), which implies that photosynthesis at the bottom of the photic layer of stratified water stations with high surface Chl *a* concentrations is close to light limitation. These situations, however, must be transient, because the development of phytoplankton blooms at the surface layers causes an increase in light attenuation, which reduces the depth of the photic layer, and phytoplankton situated close to

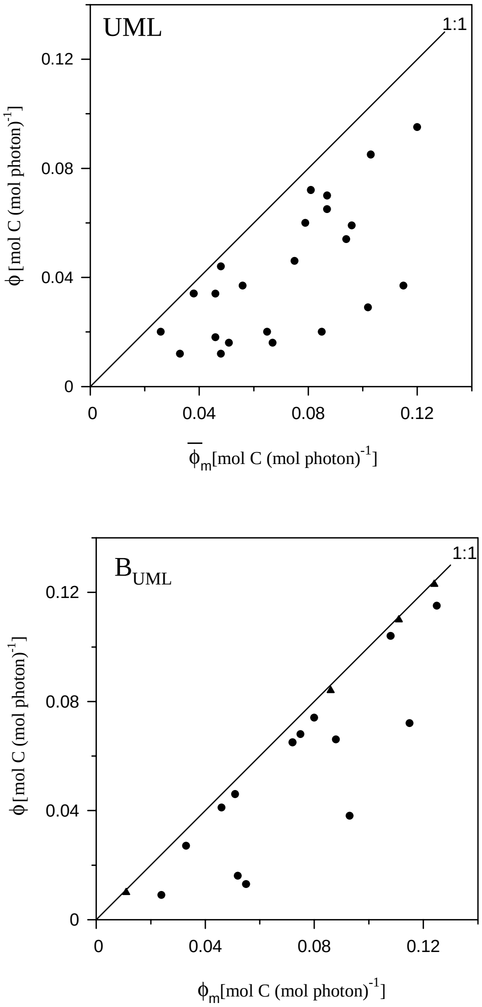

Fig. 4. Depth-averaged maximum quantum yield versus average in situ quantum yield in the upper mixer layer (UML) and single values of operational quantum yields versus maximum quantum yields below the UML (B_{UML}). Triangles correspond to samples from B_{UML} of stations 156, 169, 177 and 178 in the Gerlache Strait, which were close to be light-limited.

the 1% light level will be left with insufficient light for photosynthesis.

3.6. Primary production and phytoplankton growth rates

PP values ranged from 0.6 to 3.5 g C m^{-2} d^{-1} (Table 4) and were comparable to those recorded in upwelling systems such as the Benguela (0.5–4 g C m^{-2} d^{-1}; Brown and Field, 1986; Estrada and Marrasé, 1987; Brown et al., 1991), Peru (1.9 g C m^{-2} d^{-1}; Barber and Smith, 1981), California (0.5–2.6 g C m^{-2} d^{-1}; Pilskaln et al., 1996) and NW Iberian peninsula (0.8–2.4 g C m^{-2} d^{-1}; Tilstone et al., 1999). TWW waters showed the lowest values, which were different from those of the other two water masses ($0.001 \leqslant P \leqslant 0.004$). The highest values were found in BCW and BWW, with no differences between them ($P = 0.47$). The differences in primary production were associated with differences in Chl *a* concentration and photosynthetic parameters (Table 1). The phytoplankton composition was also different; large forms (> 10 μm) dominated BCW and BWW, while the phytoplankton community of TWW was dominated by *Cryptomonas* sp. (Varela et al., 2002). Our primary production values were consistently higher than those of Varela et al. (2002), a result that may arise from the different methodologies employed. The 24-h incubations used by Varela et al. (2002) can cause loss of fixed carbon through respiration at night and by grazing of protozoa and, therefore, should give an estimation closer to net than to gross production. In contrast, our estimates were based on short incubations, which are closer to gross than to net production (Williams, 1993; Joint et al., 2002). Our data confirm that the Gerlache Strait (BCW waters) is a region of high primary production (Holm-Hansen and Mitchell, 1991), but also support the recent evidence that Antarctic frontal regions (BWW waters) must be considered as high primary production sites (Boyd et al., 1995; Jochem et al., 1995; Park et al., 1999), an observation that might partially explain the paradox of apparent low primary production of the Southern Ocean and its food webs dynamics (Priddle et al., 1986; El-Sayed, 1987). In fact, the Southern Ocean is viewed as a mosaic of subsystems, where some are highly productive whereas others have lower primary production with long periods of dominant heterotrophy (Treguer and Jacques, 1992).

Table 4
Integrated primary production in the three water bodies[a]

BCW		BWW		TWW	
Station	g C m^{-2} d^{-1}	Station	g C m^{-2} d^{-1}	Station	g C m^{-2} d^{-1}
34	3.08	12	3.02	1	1.91
39	1.53	15	3.49	5	0.56
40	2.92	17	1.78	8	0.88
47	1.51	24	1.57	79	0.57
156	3.58	29	3.52	81	0.95
168	1.11			94	0.94
169	2.76			97	0.53
177	2.40			121	2.90
178	0.73			123	0.68
184	3.16			138	0.91
				140	1.19
				142	1.24
Mean	2.28 ± 0.98		2.68 ± 0.94		1.11 ± 0.68

[a] BCW, Bellingshausen cold waters; BWW, Bellingshausen warm waters; TWW, transitional Weddell waters.

Carbon-specific gross growth rates in the UML (Table 5) varied from 0.15 to 0.76 (d^{-1}), which correspond to 0.22 and 1.09 doublings d^{-1}, respectively, and are similar to those reported by Spies (1987) for summer microplankton populations from the Weddell Sea. The mean growth rate in the UML of BCW ($0.54 \pm 0.20\ d^{-1}$) was slightly higher and significantly different ($0.03 \leqslant P \leqslant 0.06$) than those of BWW ($0.35 \pm 0.09\ d^{-1}$) and TWW ($0.37 \pm 0.08\ d^{-1}$). The mean growth rates in TWW and BWW were not different ($P = 0.63$). The overall mean growth rate in UML ($0.43 \pm 0.16\ d^{-1}$, Table 5) was also similar to the carbon-based estimate ($0.41 \pm 0.23\ d^{-1}$) given by Smith et al. (1999). Our growth rates for UML are comparable to those reported for temperate seas (e.g., Cullen et al., 1992; Marañón et al., 2000) and suggest that Antarctic phytoplankton is well adapted to its environmental conditions.

The mean growth rate ($0.20 \pm 0.19\ d^{-1}$) in B_{UML} (Table 6) was significantly lower than that of the UML ($P < 0.001$), but there were no differences

Table 5
Carbon-specific gross rates and doublings per day in the upper mixer layer (UML) in the three water bodies[a]

Station	Water bodies	Z_{UML} (m)	μ (d^{-1})	k (doublings d^{-1})
5	TWW	10	0.55	0.79
8	TWW	37	0.38	0.55
12	BWW	47	0.44	0.64
15	BWW	41	0.31	0.45
17	BWW	78	0.32	0.46
24	BWW	47	0.23	0.33
29	BWW	32	0.43	0.62
34	BCW	17	0.76	1.09
39	BCW	6	0.69	1.00
40	BCW	35	0.36	0.52
47	BCW	8	0.46	0.66
79	TWW	17	0.37	0.53
81	TWW	47	0.29	0.42
97	TWW	7	0.34	0.49
121	TWW	50	0.29	0.42
123	TWW	47	0.33	0.48
140	TWW	7	0.41	0.59
142	TWW	23	0.36	0.52
156	BCW	10	0.52	0.75
168	BCW	40	0.15	0.22
169	BCW	4	0.75	1.08
177	BCW	6	0.59	0.85
184	BCW	3	0.58	0.84
		Mean	0.43±0.16	0.62±0.23

[a] At the bottom mean and standard deviation for all samples. Depths of UML (Z_{UML}) are also given.

Table 6
Carbon-specific gross rates and doublings per day below the upper mixer layer (B_{UML}) in the three water bodies[a]

Station	Water bodies	Z (m)	μ (d^{-1})	k (doublings d^{-1})
1	TWW	8	0.54	0.78
1	TWW	23	0.07	0.10
5	TWW	18	0.14	0.20
39	BCW	11	0.23	0.34
79	TWW	20	0.09	0.14
94	TWW	5	0.39	0.56
94	TWW	20	0.11	0.16
97	TWW	16	0.14	0.21
138	TWW	5	0.36	0.52
140	TWW	20	0.07	0.11
156	BCW	15	0.22	0.31
156	BCW	30	0.02	0.03
169	BCW	5	0.56	0.81
169	BCW	30	0.01	0.01
177	BCW	18	0.05	0.08
178	BCW	5	0.51	0.74
178	BCW	20	0.01	0.02
184	BCW	10	0.11	0.16
		Mean	0.20±0.19	0.29±0.27

[a] At the bottom mean and standard deviation for all samples. Depths of sampling are also given.

between growth rates in the B_{UML} of BCW and those in TWW ($P = 0.81$). Growth rates in this layer varied between 0.01 and 0.56 d^{-1} with the lowest values corresponding to those samples from the bottom of the photic layers (Table 6), where light limitation of photosynthesis could occur (see also Fig. 4). The highest values, which were even greater than the mean of UML, were found at shallower samples (Table 6) where photosynthesis was clearly light-saturated (Fig. 4).

4. Conclusions

The study of photosynthetic parameters in the western Bransfield Strait, Gerlache Strait, and southern part of the Bellingshausen Sea confirms that phytoplankton photosynthesis is not light-limited in the UML. There was some evidence of light limitation at the bottom of the photic layer, caused by the phytoplankton bloom development in coastal stratified regions, which is often a transient event. A comparison of photosynthetic parameters between the three different water bodies showed that Bellingshausen cold waters (BCW) and Bellingshausen warm waters (BWW) were similar and different from Bransfield waters (TWW). The high maximum quantum yields found in the three water bodies suggest that iron limitation did not occur in this region. Primary production was high in the Gerlache Strait (BCW) and in the front that separated BCW and TWW from BWW, and comparable to that of upwelling system of temperate waters, which indicates that frontal areas will be included in the high productivity regions of the Southern Ocean, together with marginal ice zones and shelf waters. Carbon-specific growth rates in the UML were high and similar to non-nutrient and non light-limited temperate seas. Consequently, if light and iron are not limiting photosynthesis in this region, the control of phytoplankton biomass should be due to other factors. Microzooplankton grazing could be one of these factors, as indicated by Klaas (1997) and also suggested by the differences between primary production estimated from short and 24-h incubations. In contrast, the role of mesozooplankton is rather weak. Previous (Alcaraz et al., 1998), and parallel studies (Cabal et al., 2002) in the zone indicate that zooplankton grazed between 0.08% and 0.14% of chlorophyll standing stocks and between 0.9% and 25% of daily primary production. Sinking seemed to be also important during blooms of large phytoplankton (Serret et al., 2002).

Acknowledgements

The authors thank to the technical staff, officers and crew of R/V *Hespérides* in ensuring the success of cruise FRUELA 95. The authors are also grateful to all the participants in cruise FRUELA 95. Special thanks to R. Varela for help with the absorption spectra, to C.G. Castro for general comments and T. Rellan for providing maps and figures. A fellowship from the Spanish Ministerio de Educación y Ciencia allowed L.M.L. to carry out this work. B.A. was funded by a post-graduate grant from CSIC-Xunta de Galicia, and G.H.T. by a fellowship from the European Commission MAST programme (MAS3-CT96-5022). This research was supported by the CICYT (Spanish Commission of Science and Technology) project ANT94-1010.

References

Alcaraz, M., Saiz, E., Fernandez, J.A., Trepat, I., Figueiras, F.G., Calbet, A., Bautista, B., 1998. Antarctic zooplankton metabolism: carbon requirements and ammonium excretion of salps and crustacean zooplankton in the vicinity of the Bransfield Starit during January 1994. Journal of Marine Systems 17, 347–359.

Arbones, B., Figueiras, F.G., Zapata, M., 1996. Determination of phytoplankton absorption coefficient in natural seawater samples: evidence of a unique equation to correct the pathlength amplification on glass-fiber filters. Marine Ecology Progress Series 137, 293–304.

Barber, R.T., Smith, R.L., 1981. Coastal upwelling ecosystems. In: Longhurst, A.R. (Ed.), Analysis of Marine Ecosystems. Academic press, New York, pp. 31–68.

Boyd, P.W., Robinson, C., Savidge, G., Williams, P.J., 1995. Water column and sea-ice primary production during Austral spring in the Bellingshausen Sea. Deep-Sea Research II 42, 1177–1200.

Brown, P.C., Field, J.G., 1986. Factors limiting phytoplankton production in a nearshore upwelling area. Journal of Plankton Research 8, 55–68.

Brown, P.C., Painting, S.J., Cochraine, K.L., 1991. Estimates of phytoplankton and bacterial biomass and production in the northern and southern Benguela ecosystems. South African Journal Marine Science 11, 537–564.

Cabal, J.A., Alvarez-Marqués, F., Acuña, J.L., Quevedo, M., González-Quirós, R., Huskin, I., Fernández, D., Rodriguez del Valle, C., Anadon, R., 2002. Mesozooplankton distribution and grazing during the productive season in the Northwest Antarctic Peninsula (FRUELA cruises). Deep-Sea Research II 49, 869–882.

Castro, C.G., Ríos, A.F., Doval, M.D., Pérez, F.F., 2002. Nutrient utilisation and chlorophyll distribution in the Atlantic sector of the Southern Ocean during Austral summer 1995–96. Deep-Sea Research II 49, 623–641.

Cleveland, J.S., Perry, M.J., Kiefer, D.A., Talbot, M.C., 1989. Maximal quantum yield of photosynthesis in the northwestern Sargasso Sea. Journal of Marine Research 47, 869–889.

Cullen, J.J., Lewis, M.R., Davis, C.O., Barber, R.T., 1992. Photosynthetic characteristics and estimated growth rates indicate grazing is the proximate control of primary production in the Equatorial Pacific. Journal of Geophysical Research 97, 639–654.

Doval, M.D., Álvarez-Salgado, X.A., Castro, C.G., Pérez, F.F., 2002. Dissolved organic carbon distributions in the Bransfield and Gerlache Straits, Antarctica. Deep-Sea Research II 49, 663–674.

Dubinsky, Z., 1980. Light utilization efficiency in natural phytoplankton communities. In: Falkowski, P.G. (Ed.), Primary Productivity in the Sea. Plenum Press, New York, London, p. 531.

El-Sayed, S.Z., 1987. Biological productivity of Antarctic waters: present paradoxes and emerging paradigms. In: El-Sayed, S.Z., Tomo, A.P. (Eds.), Antarctic Aquatic Biology. SCAR, Cambridge, England, pp. 1–21.

El-Sayed, S.Z., 1988. Productivity of the Southern ocean: a closer look. Comparative Biochemistry and Physiology 90, 489–498.

Estrada, M., Marrasé, C., 1987. Phytoplankton biomass and productivity off the Namibian coast. In: Payne, A.I.L., Gulland, J.A., Brink, K.H. (Eds.), The Benguela and Comparable Ecosystems. South African Journal Marine Science 5, 347–356.

Falkowski, P.G., Raven, J.A., (Eds.), 1997. Light Absorption and Energy Transfer in the Photosynthetic Apparatus. In: Aquatic Photosynthesis. Blackwell Science, Oxford, pp. 33–64.

Figueiras, F.G., Pérez, F.F., Pazos, Y., Ríos, A.F., 1994. Light and productivity of Antarctic phytoplankton during Austral summer in an ice edge region in the Weddel-Scotia Sea. Journal of Plankton Research 16, 233–253.

Figueiras, F.G., Estrada, M., López, O., Arbones, B., 1998. Photosynthetic parameters and primary production in the Bransfield Strait: relationships with mesoscale hydrographic structures. Journal of Marine Systems 17, 129–141.

Figueiras, F.G., Arbones, B., Estrada, M., 1999. Implications of bio-optical modelling of phytoplankton in Antarctic waters: further evidence of no light limitation in the Bransfield Strait. Limnology and Oceanography 44, 1599–1608.

Garcia, M.A., Castro, C.G., Ríos, A.F., Doval, M.D., Rosón, G., Gomis, D., López, O., 2002. Water masses and distribution of physico-chemical properties in the Western Bransfield Strait and Gerlache Strait during Austral summer 1995/96. Deep-Sea Research II 49, 585–602.

Harrison, W.G., Platt, T., 1986. Photosynthetis-irradiance relationships in polar and temperate phytoplankton populations. Polar biology 5, 153–164.

Helbling, E.W., Villafane, V.E., Holm-Hansen, O., 1995. Variability of phytoplankton distribution and primary production around Elephant Island, Antarctica, during 1990–1993. Polar Biology 15, 233–246.

Holm-Hansen, O., Mitchell, B.G., 1991. Spatial and temporal distribution of phytoplankton and primary production in the western Bransfield Strait region. Deep-Sea Research II 38, 961–980.

Holm-Hansen, O., Mitchell, B.G., Hewes, C.D., Karl, D.M., 1989. Phytoplankton blooms in the vicinity of Palmer Station. Polar Biology 10, 49–57.

Jochem, F.J., Mathot, S., Quéguiner, B., 1995. Size-fractioned primary production in the open Southern Ocean in Austral spring. Polar Biology 15, 381–392.

Joint, I., Chou, L., Figueiras, F.G., Gromm, S., Loijens, M., Tilstone, G., Wollast, R., 2002. The response of phytoplankton production to periodic upwelling and relaxation events at the Iberian shelf break. Progress in Oceanography, submitted for publication.

Kirk, J.T.O., 1983. Light and Photosynthesis in Aquatic Ecosystems. Cambridge University Press, Cambridge, pp. 401.

Kishino, M., Takahashi, N., Okami, N., Ichimura, S., 1985. Estimation of the spectral absorption coefficients of phytoplankton in the sea. Bulletin of Marine Science 37, 634–642.

Klaas, C., 1997. Microprotozooplankton distribution and their potential grazing impact in the Antarctic Circumpolar Current. Deep-Sea Research II 44, 375–393.

Krebs, W., 1983. Ecology of neritic marine diatoms. Arthur Harbour, Antarctica. Micropaleontology 29, 267–297.

Lindley, S.T., Bidigare, R.R., Barber, R.T., 1995. Phytoplankton photosynthesis parameters along 140°W in the equatorial Pacific. Deep-Sea Research II 42, 441–463.

Marañón, E., Holligan, P.M., Varela, M., Mouriño, B., Bale, A.J., 2000. Basin-scale variability of phytoplankton biomass, production, and growth in the Atlantic Ocean. Deep-Sea Research I 47, 825–857.

Martin, J.H., Fitzwater, S.E., Gordon, R.M., 1990. Iron deficiency limits growth in Antarctic waters. Global Biogeochemical Cycles 4, 5–12.

Mitchell, B.G., Holm-Hansen, O., 1991. Observations and modelling of the Antarctic phytoplankton crop in relation to mixing depth. Deep-Sea Research II 38, 981–1007.

Park, M.G., Yang, S.R., Kang, S.H., Chung, K.H., Shim, J.H., 1999. Phytoplankton biomass and primary production in the marginal ice zone of the northwestern Weddell Sea during Austral summer. Polar Biology 21, 251–261.

Pilskaln, C.H., Paduan, J.B., Chavez, F.P., Anderson, R.Y., Berelson, W.M., 1996. Carbon export and regeneration in the coastal upwelling system of Monterey Bay, central California. Journal Marine Research 54, 1149–1178.

Platt, T., Sathyendranath, S., Ulloa, O., Harrison, W.G., Hoepffner, N., Goes, J., 1992. Nutrient control of phytoplankton photosynthesis in the Western North Atlantic. Nature 356, 229–231.

Priddle, J., Hawes, I., Ellis-Evans, J.C., 1986. Antarctic aquatic ecosystems as habitats for phytoplankton. Biological Review 61, 199–238.

Sakshaug, E., Holm-Hansen, O., 1984. Factor governing pelagic production in polar oceans. In: Holm-Hansen, O., Bolis, L., Gilles, R. (Eds.), Marine Phytoplankton and Productivity, Lecture Notes on Coastal and Estuarine Studies. Springer-Verlag, Berlin/Heidelberg. pp. 1–18.

Sakshaug, E., Holm-Hansen, O., 1986. Photoadaptation in antarctic phytoplankton: variations in growth rate, chemical composition and P versus I curves. Journal of Plankton Research 8, 459–473.

Serret, P., Fernández, E., Anadón, R., Varela, M., 2002. Phytoplankton size and net microplankton metabolism in Western Brasfield Strait and Gerlache Strait, Antarctica: relation to biogenic carbon export. Journal Plankton Research, submitted for publication.

Smith, W.O., Sakshaug, E., 1990. Polar phytoplankton. In: Polar Oceanography. Part B: Chemistry, Biology and Geology. Academic Press, New York, pp. 477–517.

Smith, W.O., Nelson, D.M., Mathot, S., 1999. Phytoplankton growth rates in the Ross Sea, Antarctica, determinate by independent methods: temporal variations. Journal of Plankton Research 21, 1519–1536.

Spies, A., 1987. Growth rates of Antarctic marine phytoplankton in the Weddell Sea. Marine Ecology Progress Series 41, 267–274.

Sullivan, C.W., Arrigo, K.R., McClain, C.R., Comiso, J.C., Firestone, J., 1993. Distribution of phytoplankton blooms in the Southern Ocean. Science 262, 1832–1837.

Thomas, D.N., Baumann, M.E.M., Gleitz, M., 1992. Efficiency of carbon assimilation and photoacclimation in a small unicellular *Chaetoceros* species form the Weddell Sea (Antarctica): influence of temperature and irradiance. Journal of Experimental Marine Biology and Ecology 157, 195–209.

Tilstone, G.H., Figueiras, F.G., Fermín, E.G., Arbones, B., 1999. Significance of nanophytoplankton photosynthesis and primary production in a coastal upwelling system (Ría de Vigo, NW Spain). Marine Ecology Progress Series 183, 13–27.

Tilzer, M.M., von Bodungen, B., Smetacek, V., 1985. Light-dependence of phytoplankton photosynthesis in the Antarctic Ocean: implications for regulating productivity. In: Siegfried, W.R., Condy, P.R., Laws, R.M. (Eds.), Antarctic Nutrient Cycles and Food Webs. Springer-Verlag, Berlin/Heidelberg, pp. 60–69.

Tokarczyk, R., 1987. Classification of water masses in the Bransfield Strait and Southern part of the Drake Passage using a method of statistical multidimensional analysis. Polish Polar Research 8, 333–366.

Treguer, P., Jacques, G., 1992. Dynamics of nutrients and phytoplankton, and fluxes of carbon, nitrogen and silicon in the Antarctic Ocean. Polar Biology 12, 149–162.

Varela, M., Fernandez, E., Serret, P., 2002. Size-fractionated phytoplankton biomass and primary production in the Gerlache and south Bransfield Straits (Antarctic Peninsula) in Austral summer 1995–1996. Deep-Sea Research II 49, 749–768.

Webb, W.L., Newton, M., Starr, D., 1974. Carbon dioxide exchange of *Alnus rubra*: a mathematical model. Oecologia 17, 281–291.

Williams, P.J.LeB., 1993. Chemical and tracer methods of measuring plankton production. ICES Marine Science Symposium 197, 20–36.

Yentsch, C.S., Menzel, D.W., 1963. A method for the determination of phytoplankton chlorophyll and phaeophytin by fluorescence. Deep-Sea Research 10, 221–231.